**Table 1 Nondimensional eigenvalue numbers of simply supported square plate**

| Mode, (r,s) | Number of elements per side, N | | | | | | | | Exact Solution |
|---|---|---|---|---|---|---|---|---|---|
| | 2 | | | | 4 | | | | |
| | ν = 0.0 | | ν = 0.3 | | ν = 0.0 | | ν = 0.3 | | |
| | Q Arrangement | P Arrangement | Q Arrangement | P Arrangement | Q Arrangement | P Arrangement | Q Arrangement | P Arrangement | |
| (1,1) | 386.14 | 384.94 | 378.15 | 380.13 | 388.93 | 388.74 | 386.81 | 387.47 | 389.64 |
| (1,2) | 2477.59 | 2477.59 | 2476.96 | 2476.96 | 2415.26 | 2415.26 | 2386.91 | 2386.91 | 2435.23 |
| (2,2) | 6541.94 | 6541.94 | 6541.94 | 6541.94 | 6179.56 | 6179.56 | 6090.60 | 6090.60 | 6324.18 |
| (1,3) | 7149.37<br>9922.22 | 10008.09<br>10458.52 | 7361.34<br>9967.93 | 9154.84<br>9702.58 | 9482.08<br>9704.72 | 9334.84<br>9548.69 | 9060.72<br>9499.83 | 9060.72<br>9395.30 | 9740.91 |
| (2,3) | 18181.25 | 18181.25 | 17713.33 | 17713.33 | 16144.46 | 16144.46 | 15670.75 | 15670.75 | 16462.14 |
| (3,3) | 32072.08 | 35119.77 | 29521.72 | 32609.40 | 30843.18 | 30676.12 | 29507.27 | 29477.98 | 31560.55 |

The values of the nondimensional coefficients for central deflection for different Poisson's ratios for clamped plates for both central concentrated load ($w_c D/PL^2$) and uniformly distributed loads ($w_c D/qL^4$) are tabulated in Ref. 4. The results for the $P$ mesh (see Fig. 1b) of a clamped square plate are plotted in Figs. 2 and 3. From Figs. 2 and 3, it is seen that the effect of an increase in the Poisson's ratio is to make the finite element approximation of the structure (using these elements) more flexible; and that, as the mesh is made finer and finer, the nondimensional coefficient tends to converge to the exact value for all values of $\nu$. Also, it can be noted that the percentage error in the coefficients is the least for $\nu = 0.0$.

The nondimensional eigenvalues for free vibration ($=\rho t\omega^2 L^4/D$) were evaluated for $\nu = 0.0$ and 0.3 for mesh size of $N = 2$ and $N = 4$ for the simply supported square plate. The results are shown in Table 1. Although the percentage error in the lowest eigenvalue is least when $\nu = 0.0$, the same is not true for other eigenvalues.

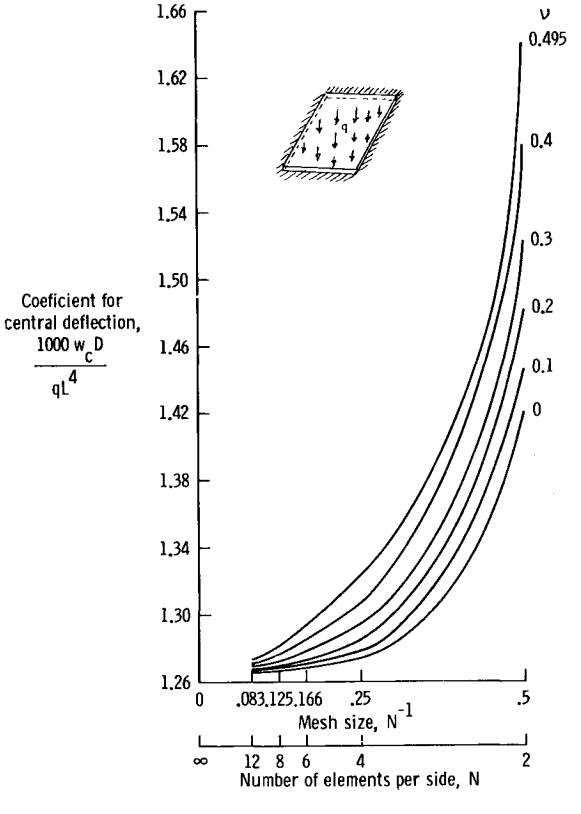


**Fig. 3 Effect of Poisson's Ratio on nonconforming quintic Element.**

Based on this study, the following conclusions about the plate-bending finite element approximations using nonconforming elements in general, and the nonconforming element of Narayanaswami[3,4] in particular, are drawn:

1) The nondimensional coefficients for central deflection of a square plate, $w_c D/PL^2$ for central concentrated load and $w_c D/qL^4$ for uniformly distributed loads are dependent on Poisson's ratio, $\nu$.

2) The nondimensional eigenvalues, $\rho t\omega^2 L^4/D$, are also dependent on Poisson's ratio, $\nu$.

3) As the finite element mesh is made finer and finer, the coefficients tend to converge to the exact value for all values of $\nu$. Convergence depends on the problem and the elements used.

### References

[1] Timoshenko, S. and Woinowsky-Krieger, S., *Theory of Plates and Shells*, 2nd ed., McGraw-Hill, New York, 1959, pp. 79–83.

[2] Cowper, G. R. et al., "A High Precision Triangular Plate-Bending Element," Aeronautical Rept. LR-514, Dec. 1968, National Research Council of Canada, Ottawa, Canada.

[3] Narayanaswami, R., "New Plate and Shell Elements for NASTRAN," TM X-2893, Sept. 1973, NASA.

[4] Narayanaswami, R., "New Triangular and Quadrilateral Plate-Bending Finite Elements," TN D-7407, April 1974, NASA.

# One-Parameter Solution of the Spanwise Rotating Blade Boundary-Layer Equation

Z. U. A. Warsi*
*Mississippi State University, Mississippi State, Miss.*

In Ref. 1 the author proposed a parametric method of solution of the spanwise boundary-layer equation for a long cylindrical blade. The one-parameter equation contained two

Received January 28, 1974; received April 1, 1974. This work has been supported in part by the Army Research Office—Durham.

Index categories: Fluid Dynamics; Boundary Layers and Convective Heat Transfer—Laminar.

* Associate Professor, Department of Aerophysics and Aerospace Engineering.

unknown functions depending on the parameter $f_1 = U'\theta_x^2/\nu$ and the distance $d$ of the axis of rotation from the origin of coordinates. If these unknown functions are tabulated in advance for each specific case then the exact solution can be obtained by the finite-difference method, starting the solution from the stagnation point. In Ref. 1 certain approximate forms of the unknown functions were prescribed and solutions of the equation were obtained by starting the solution from the point of minimum pressure, viz., $f_1 = 0$. This formulation required the positioning of the axis of rotation at such a distance from the leading edge of the blade that Fogarty's[2] solution could be used as an initial condition at $f_1 = 0$. These shortcomings have been eliminated in the present Note by separating the effects of the plane potential, centrifugal force, and the position of the axis of rotation in the manner of Rott and Smith.[3] Numerical solutions of the pertinent equations have been obtained for sufficient values of the parameter $f_1$. Once $f_1$ is determined, the solution of the spanwise equation can readily be obtained by using the plotted values.

## Analysis

The transformed spanwise boundary-layer equation for a long cylindrical blade as given in Ref. 1 [Eq. (9)] is

$$u\,\partial v/\partial x + w\,\partial v/\partial z + 2u\cos\beta(x) = U^2 + \nu\,\partial^2 v/\partial z^2 \tag{1}$$

with the boundary conditions

$$z = 0: \quad u = v = w = 0 \tag{2a}$$

$$z \to \infty: \quad u \to U(x), \quad v \to \tilde{\phi}(x) - 2\tilde{X} + K \tag{2b}$$

where $\tilde{\phi}_1(x) = \phi_1(x) - \phi_1(0)$, $U(x) = \partial\phi_1/\partial x$, $\tilde{X} = X - X_s$, and $K = \phi_1(0) + 2(d - X_s)$. Here $\phi_1(x)$ is the chordwise velocity potential due to a unit velocity at infinity and $X$ is the Cartesian distance along the chord such that the leading edge of the blade ($x = 0$) is at a distance $X_s$ from the axis $X = 0$. Further, $d$ is the chordwise distance of the axis of rotation from $X = 0$. The relation between $X$ and $x$ is

$$X = \int_0^x \cos\beta(x)\,dx + X_s$$

where $\beta(x)$ is the angle between the axis of rotation and the local surface normal.

Because of the linearity of Eq. (1), one can write $v$ in the manner of Rott and Smith[3] as the sum of three components

$$v = v_a + v_b + v_c$$

where $v_a$, $v_b$, and $v_c$ all satisfy Eq. (2a), and as $z \to \infty$,

$$v_a \to \tilde{\phi}_1(x) = \int_0^x U(x)\,dx$$

$$v_b \to -2\tilde{X}$$

$$v_c \to K$$

Introducing the functions $\chi_1$, $\chi_2$, and $\chi_3$, defined as

$$v_a = \tilde{\phi}_1\chi_1, \quad v_b = -2\tilde{X}\chi_2, \quad v_c = K\chi_3$$

in Eq. (1) and affecting the one-parameter transformation of Loitsianskii[4] as detailed in Ref. 1, we have the following equations:

$$D\chi_1^{(1)} + (U^2\theta_x^2/\nu\alpha^2\tilde{\phi}_1)[1 - \chi_1^{(1)}(\partial\phi^{(1)}/\partial\eta)] = L\chi_1^{(1)} \tag{3}$$

$$D\chi_2^{(1)} + (U\theta_x^2\cos\beta/\nu\alpha^2\tilde{X})(1 - \chi_2^{(1)})\partial\phi^{(1)}/\partial\eta = L\chi_2^{(1)} \tag{4}$$

$$D\chi_3^{(1)} = L\chi_3^{(1)} \tag{5}$$

where $D$ and $L$ are operators defined as

$$D \equiv \frac{\partial^2}{\partial\eta^2} + \frac{F^{(1)} + 2f_1}{2\alpha^2}\phi^{(1)}\frac{\partial}{\partial\eta}$$

$$L \equiv \frac{f_1 F^{(1)}}{\alpha^2}\left(\frac{\partial\phi^{(1)}}{\partial\eta}\frac{\partial}{\partial f_1} - \frac{\partial\phi^{(1)}}{\partial f_1}\frac{\partial}{\partial\eta}\right)$$

In Eqs. (3–5), the superscript (1) denotes the one-parameter approximation. If $y$ is the spanwise coordinate, $\bar{z}$ the coordinate measured normal to the surface ($\bar{z} = 0$ at the surface), and $\omega$ the uniform angular velocity of the blade, then other quantities are as follows:

$\theta_x = (\omega y)^{1/2} \times$ the chordwise momentum thickness

$\delta_x^* = (\omega y)^{1/2} \times$ the chordwise displacement thickness

$$\eta = \alpha(\omega y)^{1/2}\frac{\bar{z}}{\theta_x}, \quad u = U(x)\frac{\partial\phi^{(1)}}{\partial\eta}, \quad f_1 = \frac{U'\theta_x^2}{\nu}, \quad H^{(1)} = \frac{\delta_x^*}{\theta_x}$$

$$\zeta^{(1)} = (\theta_x/U)(\omega y)^{-1/2}(\partial u/\partial\bar{z})_{\bar{z}=0}, \quad F^{(1)} = 2[\zeta^{(1)} - (2 + H^{(1)})f_1]$$

where $\alpha = 0.47$, $\nu$ is the kinematic viscosity, and a prime denotes differentiation with respect to $x$.

The significance of the one-parameter approximation is that $f_n = U^{n-1}(d^nU/dx^n)(\theta_x^2/\nu)^n = 0$ for $n \geqq 2$. This implies that

$$(U\theta_x^2/\nu)f_1' \simeq F^{(1)}f_1 \tag{6}$$

and $U''$, $U'''$, etc., are considered negligible in the formulation of the one-parameter equations (3–5). This restriction, however, does not seem to be too restrictive because the values of $f_1$ in any actual calculation are obtained through the solution of the momentum integral equation in which $U''$ is not set equal to zero. Further, the one-parameter solutions of Loitsianskii[4] match very well with the available solutions in two dimensions.

A study of Eqs. (3–5) suggest that because of the functions

$$P_1(f_1) = U^2\theta_x^2/\nu\tilde{\phi}_1 \quad \text{and} \quad P_2(f_1) = U\theta_x^2\cos\beta/\nu\tilde{X} \tag{7}$$

the resolution of $v$ into different components $v_a$, $v_b$, and $v_c$ is not as successful as it was in the "wedge problem" of Rott and Smith.[3] If these functions can be expressed as unique functions of $f_1$ applicable to all problems, then Eqs. (3–5) can be solved once and for all.

Much analysis is needed to prescribe the universal functions $P_1$ and $P_2$. It was found that there exists a class of surfaces for which $P_1 = P_2$ at all points of the surface and for this class

$$\tilde{\phi}_1 = \gamma\tilde{X}, \quad \gamma = \text{const} \tag{8}$$

It can be immediately verified that for a flat surface $\gamma = 1$ and $P_1 = P_2 = 2\alpha^2$ throughout. Moreover, for the case of a flat plate, $(\chi_1^{(1)} - 2\chi_2^{(1)})$ satisfies the Fogarty's[2] equation. Equation (8) is also satisfied by the potential distributions for circular and elliptic cylinders with $\gamma \neq 1$ and $P_1 = P_2$ throughout the surface.

For cylinders of arbitrary sections it can be verified that $P_1 = P_2$ only at the points of stagnation ($f_1 = f_{1s}$) and of the minimum pressure ($f_1 = 0$). For arbitrary sections at $f_1 = 0$ we always have $P_1 = P_2 = \alpha^2$.

Based upon numerical experimentation and matching the results with those obtained by Fogarty[2] and Graham[5] we prescribe the following form of $P(f_1)$ for general body shapes

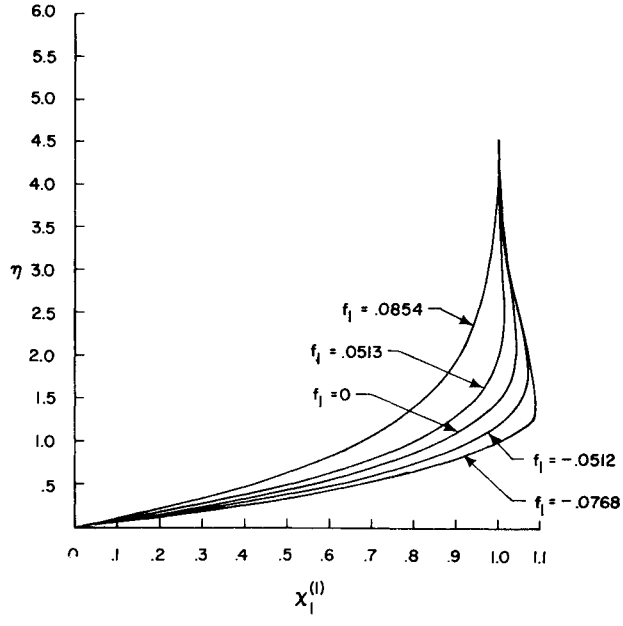


**Fig. 1 Spanwise boundary-layer profiles $\chi_1^{(1)}$ as functions of $\eta$.**

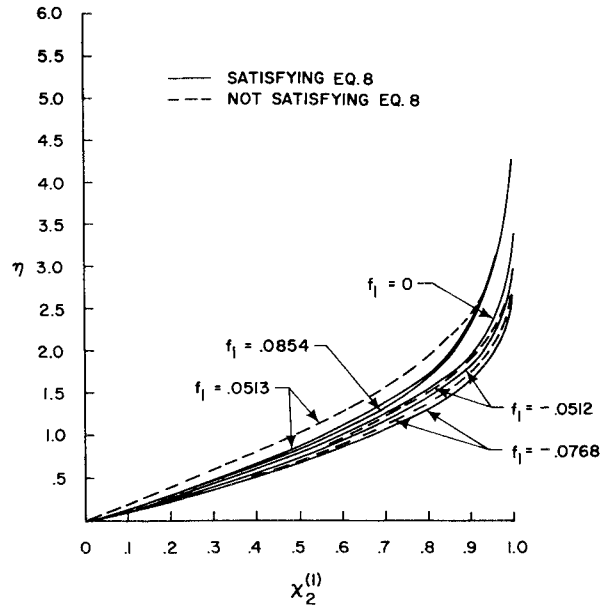


**Fig. 2 Spanwise boundary-layer profiles $\chi_2^{(1)}$ as functions of $\eta$.**

$$P_1(f_1) = \alpha^2 + (2f_1/f_{1s})(f_{1s} - \alpha^2/2), \quad -f_{1s} \leqq f_1 \leqq f_{1s} \tag{9}$$

For surfaces satisfying Eq. (8), we have $P_1(f_1) = P_2(f_1)$ where $P_1$ is defined in Eq. (9). For surfaces which do not satisfy Eq. (8), the $P_2(f_1)$ distribution is chosen as

$$P_2(f_1) = P_1(f_1) + C\alpha^2 f_1/f_{1s}[1 - (f_1/f_{1s})]^{1/2} \tag{10}$$

Good comparison with the results of Refs. 2 and 5 was obtained by taking $C = -8$ and $C = 4$ for the ranges $0 \leqq f_1 \leqq f_{1s}$ and $-f_{1s} \leqq f_1 \leqq 0$ respectively.

Equations (3–5) with $P_{1,2}(f_1)$ replacing $U^2\theta_x^2/\nu\tilde{\phi}_1$ and $U^2\theta_x^2 \cos\beta/\nu\tilde{X}$ have been solved by an implicit finite-difference method for values of $f_1$ in the range $-f_{1s} \leqq f_1 \leqq f_{1s}$, where $f_{1s} = 0.0854$. In this range the tabulated values of $\partial\phi^{(1)}/\partial\eta$ are available in Ref. 4. The boundary conditions for Eqs. (3–5) are

$$\eta = 0: \ \chi_1^{(1)} = \chi_2^{(1)} = \chi_3^{(1)} = 0$$

$$\eta \to \infty: \ \chi_1^{(1)}, \chi_2^{(1)}, \text{ and } \chi_3^{(1)} \to 1$$

Initial conditions were prescribed at $f_1 = f_{1s}$ where $\chi_1^{(1)}$, $\chi_2^{(1)}$, and $\chi_3^{(1)}$ satisfy the ordinary differential equations whose solutions are known.

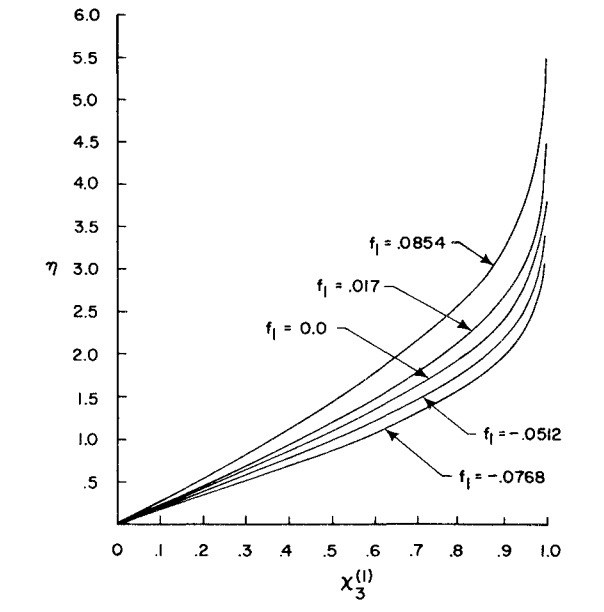


**Fig. 3 Spanwise boundary-layer profiles $\chi_3^{(1)}$ as functions of $\eta$.**

Figures 1–3 represent the values of $\chi_1^{(1)}$, $\chi_2^{(1)}$, and $\chi_3^{(1)}$ for various values of $f_1$. Tabulated values of the chordwise velocity distributions are avilable in Ref. 4. In any practical problem one has only to prescribe the nondimensional external velocity $U(x)$ and then the values of $f_1$ are obtained by the recurrence relation [Eqs. (21) and (22) of Ref. 1]

$$U^b Z^*(x_n) = U^b(x_{n-1}) Z^*(x_{n-1}) + (a + \varepsilon_{n-1}) \int_{x_{n-1}}^{x_n} U^{b-1}(x)\,dx \tag{11}$$

where $Z^* = \theta_x^2/\nu$ and $a = 0.4408$, $b = 5.714$. The function $\varepsilon_{n-1} = \varepsilon_{n-1}(f_1)$ is plotted in Ref. 1.

### Results and Discussion

The universal solutions of the rotating blade boundary-layer equations are presented for blades of sufficiently long spans. These solutions can be used for a quick and direct assessment of the velocity distribution on a given blade. The steps are as follows: 1) For a given external velocity distribution first nondimensionalize and normalize as given in Eq. (2b). 2) Prepare the table for $Z^*(x)$; Eq. (11). 3) Check to see whether Eq. (8) is satisfied. For this case, data of Fig. 1, Fig. 2 (continuous lines), and Fig. 3 have to be used. 4) If Eq. (8) is not satisfied, then Fig. 1, Fig. 2 (broken lines), and Fig. 3 have to be used.

### References

[1] Warsi, Z. U. A., "Further Theoretical Investigation of the Laminar Boundary Layer over Rotating Blades and Yawed Infinite Wings," *AIAA Journal*, Vol. 7, No. 4, April 1969, pp. 687–693.

[2] Fogarty, L. E., "The Laminar Boundary Layer on a Rotating Blade," *Journal of the Aeronautical Sciences*, Vol. 18, No. 4, April 1951, pp. 247–252.

[3] Rott, N. and Smith, W. E., "Some Examples of Laminar Boundary Layer Flow on Rotating Blades," *Journal of the Aeronautical Sciences*, Vol. 23, No. 11, Nov. 1956, pp. 991–996.

[4] Loitsianskii, L. G., "The Universal Equations and Parametric Approximations in the Theory of the Laminar Boundary Layers," *PMM*, Vol. 29, No. 1, 1965, pp. 74–92.

[5] Graham, M., "Calculation of Laminar Boundary Layer Flow on Rotating Blades," Ph.D. thesis, Sept. 1954, Cornell University, Ithaca, N.Y.

# Postbuckling Behavior of Clamped Skew Plates

M. S. S. PRABHU* AND S. DURVASULA†
*Indian Institute of Science, Bangalore, India*

POSTBUCKLING behavior of skew plates has not received adequate attention. Recently, Ref. 1 dealt with the postbuckling behavior of orthotropic skew plates. However, the results presented therein exhibit some incorrect trends. In a study of the postbuckling behavior of isotropic clamped skew plates, we were interested in examining the use of two alternative schemes in solving the problem. The first one is the Galerkin method with the Newton-Raphson (N-R) procedure, and the second is the Perturbation method. Some of the results of this investigation are reported briefly in this Note.

Received January 29, 1974; revision received May 7, 1974.
Index category: Structural Stability Analysis.

* Formerly Research Student, Department of Aeronautical Engineering; presently Engineer, Indian Scientific Satellite Project, Bangalore.
† Associate Professor, Department of Aeronautical Engineering.